Power spectrum of hadronic multiparticle rapidity distributions

P. Carruthers and T. Hakioğlu
Department of Physics, University of Arizona, Tucson, Arizona 85721
(Received 11 September 1991)

We discuss issues that arise in studying the power spectrum of rapidity histograms. These questions exist because the correlation functions are typically nontranslation invariant and confined to a finite kinematical interval. It is noted that the event density $\hat{\rho}$ referred and normalized to the average single-particle density ρ_1, leads to (normalized) factorial cumulant bin moments dependent only on the k parameter appearing in the special case of the negative-binomial distribution. An averaged two-particle correlation function is proposed to implement the purpose of the usual Wiener-Khinchin theorem. We then generalize the bin-averaged factorial-moment technique and strip-domain moment approaches to encompass power-spectra methods. The latter connect naturally to the correlation dimensions of fractal sets and evade the problems of nonstationarity at the price of increased computational complexity. Numerical examples of chaotic time series are used to generate data. Their power spectra possess distinct properties in Gaussian and intermittent dynamics. Event averaging smooths out the power spectrum of the Gaussian dynamics, whereas the nontrivial dynamical fluctuations survive the same averaging. We argue that statistically independent events can be generated by uniformly reshuffling the rapidity histograms only if fluctuations themselves are dominantly statistical. In the presence of strongly intermittent dynamical fluctuations, correlations may exist *between* different events when the event points are generated by a deterministic map. In the Appendix we give the recipe for generalizing the Wiener-Khinchin theorem to calculate the power spectrum of higher-order correlations.

PACS number(s): 13.85.Hd, 05.45.+b, 12.40.Ee

I. INTRODUCTION

Event histograms of multiparticle spectra in momentum space are highly irregular. In order to analyze the hidden patterns in a large collection of events one usually employs number density correlation functions and cumulant correlations, the latter defined to remove background correlations of lower order [1–3]. Given the hierarchy of density correlations it is possible to give various descriptions of the texture of a characteristic dynamics. Observables are defined in terms of the moments and cumulants of particle number. These moments and cumulants are integrated versions of the density correlations in proper domains of the rapidity space. Integration over a tube, or "strip," leads to correlation integrals [4,5] and to factorial moments [6,7] that can lead for high resolution to a scaling behavior corresponding to fractal structures [8–10]. In fact these methods are closely related [11].

The classic analysis of the irregularities of a signal is through the use of Fourier transform. The textbook case involves a "stationary" (time-translation-invariant) signal $x(t)$ defined in a time interval much longer than the largest correlation length present in $x(t)$. Subtracting away the background constant $\langle x(t)\rangle$ we can inspect the Fourier transform $x(\omega)$ for peaks corresponding to, for example, weak harmonic components buried in a noisy background. More important for our purposes is the Wiener-Khinchin theorem [12] which allows the construction of the (auto)correlation function from the "power spectrum" $|x(\omega)|^2$:

$$\Gamma(\tau)\equiv\langle x(t)x(t+\tau)\rangle=\int_{-\infty}^{\infty}\frac{d\omega}{2\pi}e^{-i\omega\tau}\langle|x(\omega)|^2\rangle\ . \tag{1.1}$$

Here the angular brackets indicate an ensemble average over representative configurations or a suitably long (i.e., rather longer than the largest correlation time) time average.

In order to apply the power-spectrum approach to hadronic data we must overcome two difficulties: not only is the single-particle density kinematically confined to a finite volume in phase space, but the density as well as the two-particle correlation function violate translation invariance at most energies of current interest. Perhaps because of this, the only published work known to us applying power-spectrum methods to multihadron final states is that of Takagi [13]. As is common in this field, we suppress the transverse momentum of the final-state particles and describe the event by a collection of one-dimensional rapidity variables [14] $y_1,y_2,\ldots,y_n$.

Consider the single-particle spectrum $\hat{\rho}$. For the ideal resolution it is a sum of delta functions

$$\hat{\rho}(y,\mathbf{s})=\sum_i\delta(y-s_i)\ . \tag{1.2}$$

For the finite resolution (1.2) is represented as a histogram, to be compared with the ensemble average $\rho_1(y)$. Using standard probability theory, $\rho_1(y)$ can be written in the form [2]

$$\rho_1(y)\equiv\langle\rho_1(y)\rangle \equiv\sum_n p_i n\int\sum_{j=1}^{n}ds_j\,Q_n(s_1,s_2,\ldots,s_n)\hat{\rho}(y,\mathbf{s})\ , \tag{1.3}$$

where Q_n is the joint probability to find n particles at $s_1,\ldots,s_n$ and p_n is the probability to find the system

with n particles. Figure 1 illustrates the typical appearance of an event histogram as compared with the smoothed $\rho_1(y)$. The first problem is to determine how to compare the fluctuating histograms with the smooth background. In Ref. [13] the power spectrum of $\hat{\rho}-\rho_1$ was studied. However, in many cases we recommend using instead the normalized density

$$\hat{r}(y)=\frac{\hat{\rho}(y)-\rho_1(y)}{\rho_1(y)} . \tag{1.4}$$

As explained in Sec. II, the fluctuations as measured by normalized factorial cumulant moments of all orders become independent of bin location using Eq. (1.4); therefore the central region relative fluctuations are the same as for the ends, to the extent that the negative-binomial parameter k is independent of the bin location. We later define quasistationary distributions as the weak limit of nonstationary distributions. Then the manifestation of this limit of the quasistationary in terms of the hierarchy of correlation lengths is discussed. If such conditions are met, it is possible to replace the exact correlation functions by the ones that are averaged over the c.m. variable. In Sec. III we change the phase-space-integration domain of correlation function to correspond to both bin averaging (leading usually to factorial moments) and strip averaging (leading to pair counting). By injecting Fourier generalizations in these formulations we obtain a new probe of the correlation function structure. Since it has turned out that the measured moments are not especially sensitive to the details of the correlation function [4], this approach may be of practical utility, expressing the essence of the Wiener-Khinchin theorem in a form closely related to current data analysis. In Sec. IV we simulate "data" using chaotic maps, considering the associated power spectra. Following a general discussion and summary in Sec. V, the extension of the Wiener-Khinchin theorem to higher-order correlations is discussed in the Appendix. It is also shown that correlations with fluctuating multiplicity are mainly dominated by the single-particle multiplicity fluctuations; thus the effects of fixed multiplicity fluctuations are sometimes negligible [2].

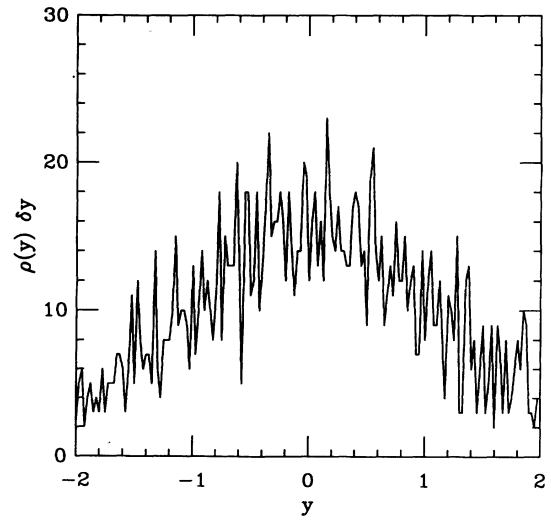

FIG. 1. A typical event histogram $\hat{\rho}(y)$.

II. RAPIDITY POWER SPECTRUM AND TWO-PARTICLE CORRELATIONS

The idealized two-particle correlation operator analogous to Eq. (1.2) is

$$\hat{\rho}_2(y_1,y_2;\mathbf{s})=\sum_{i\neq j}\delta(y_1-s_i)\delta(y_2-s_j) , \tag{2.1}$$

where the restriction $i\neq j$ is appropriate for a population of identical particles. The density-density correlation function $\rho_2(y_1,y_2)$ is constructed exactly as in (1.3). We also use the cumulant correlation function $C_2(y_1,y_2)$ defined by

$$C_2(y_1,y_2)\equiv\rho_2(y_1,y_2)-\rho_1(y_1)\rho_1(y_2) \tag{2.2}$$

and its normalized counterpart

$$R_2(y_1,y_2)=\frac{\rho_2(y_1,y_2)-\rho_1(y_1)\rho_1(y_2)}{\rho_1(y_1)\rho_1(y_2)} . \tag{2.3}$$

Clearly the nonvanishing of C_2 implies the existence of true correlations. The systematic procedure for carrying this out to all orders of correlation is summarized in Ref. [2]. We see directly from Eqs. (1.3), (1.4), and (2.3) the identity

$$\langle :\hat{r}(y_1)\hat{r}(y_2):\rangle\equiv R_2(y_1,y_2) , \tag{2.4}$$

where the colon indicates exclusion of overlapping particle indices in the product; this operation has the same effect as normal ordering for second-quantized number operators.

We now integrate y_1 and y_2 over identical bins Ω_i of width δy, the latter being sufficiently small that ρ_1 is constant over the bin. Then from (2.1) and (2.3) we find

$$\frac{1}{(\delta y)^2}\int_{\Omega_i}dy_1\int_{\Omega_i}dy_2\,R_2(y_1,y_2)=\frac{\langle n_i(n_i-1)\rangle-\langle n_i\rangle^2}{\langle n_i\rangle^2} . \tag{2.5}$$

For Poissonian bin statistics (2.5) vanishes (no correlation); for negative binomials (NB's), the right-hand side is $1/k(\delta y)$, where k is the parameter entering the NB's

$$P_n^k=\frac{(n+k-1)!}{n!(k-1)!}\frac{(\bar{n}/k)^n}{(1+\bar{n}/k)^{n+k}} . \tag{2.6}$$

The δy and c.m. energy $\sqrt{s}$ dependence of k is by now well known [15,16]. The point here is that at collider energies it is independent of the chosen bin i. In pth order the analogous result is $\int_{\Omega_i}dy_1,\ldots,dy_pR_p/(\delta y)^p=(p-1)!/k^{p-1}$, also independent of i. Therefore, the reduced cumulants, of which (2.3) is the simplest nontrivial example, treat all bin fluctuations on an equal basis for Poissonian statistics (trivial) and negative binomials (nontrivial).

Now expand $\hat{\rho}(y)$ in a Fourier series for the full rapidity interval $-Y\leq y\leq Y$:

$$\hat{\rho}(y,\mathbf{s})=\frac{1}{2Y}\sum_q \hat{\rho}_q(\mathbf{s})e^{iqy}\ ,$$
$$\hat{\rho}_q(\mathbf{s})=\int_{-Y}^{Y}dy\,\hat{\rho}(y)e^{-iqy}=\sum_j e^{-iqs_j}\ . \tag{2.7}$$

Except for normalizations and a factor of -1, the same relations hold for $\hat{r}$. We can imagine $\hat{\rho}(y)$ to be periodic with period $2Y$; the allowed q values are $\pi n/Y$, n ranging over $-\infty<n<\infty$. Now define the power spectrum $\Gamma(q,Y)$ averaged over the full rapidity interval:

$$\Gamma(q,Y)\equiv\langle:|\hat{r}_q(\mathbf{s})|^2:\rangle \tag{2.8}$$
$$\Gamma(q,Y)=\frac{1}{2Y}\int_{-Y}^{Y}dy_1\int_{-Y}^{Y}dy_2\,R_2(y_1,y_2)e^{iq(y_1-y_2)}\ . \tag{2.9}$$

In the case of translation invariance and Y sufficiently large, one passes to coordinates $\eta=(y_1+y_2)/2$ and $\zeta=y_2-y_1$, obtaining the inverse of Eq. (1.1).

Although R_2 is in general not translation invariant it is useful to consider its dependence on η and ζ (Fig. 2). Lines of fixed η and ζ are rotated 45° with respect to y_1 and y_2. In order to illustrate this point we replace ρ_2 by the uncorrelated form $\rho_1(y_1)\rho_1(y_2)$, defining

$$\Delta(\eta)=\int_{-Y}^{Y}dy_1\int_{-Y}^{Y}dy_2\,\rho_1(y_1)\rho_1(y_2)\times\delta\left[\eta-\frac{y_1+y_2}{2}\right]\ . \tag{2.10}$$

Essentially $\Delta(\eta)$ is the density of points y_1 and y_2 for a fixed c.m. value η. For the simplest case of constant density, $\rho_1(y)=1/2Y$,

$$\Delta(\eta)=\theta(Y-|\eta|) \tag{2.11}$$

describing the most desirable case of manifest translational invariance in the full rapidity range. However, in most cases the one-particle rapidity distribution can be fitted to a Gaussian,

$$\rho_1(y)\propto\exp(-y^2/\sigma^2)\ , \tag{2.12}$$

in which case $\Delta(\eta)$ becomes

$$\begin{aligned}\Delta(\eta)&\propto\int_{-Y}^{Y}d\zeta\int_{\eta-|\zeta|}^{\eta+|\zeta|}dR\,\exp(-\zeta^2/2\sigma^2-2R^2/\sigma^2)\\&=\frac{4\sigma}{4Y^2}(1-e^{-Y/4\sigma})\exp(-2\eta^2/\sigma^2)\\&\propto\frac{1}{Y}\exp(-2\eta^2/\sigma^2)\quad\text{for }\sigma\gg Y\end{aligned} \tag{2.13}$$

which is a very small variation since $\eta\le Y$. A simple fit to data is a double Gaussian, uncorrelated in η and ζ:

$$R_2(y_1,y_2)=\exp[-(y_1+y_2)^2/\sigma^2-(y_1-y_2)^2/\xi^2]\ . \tag{2.14}$$

Empirically R_2 is small when $\zeta>|\zeta|$, although η dependence remains. Schematic contours of this function appear in Fig. 3. Consulting Fig. 2 we write

$$\Gamma(g,Y)=\int_{-Y}^{Y}d\zeta\,\bar{R}_2(Y,\zeta)e^{-iq\zeta}\ , \tag{2.15}$$
$$\bar{R}_2(Y,\zeta)=\int_{-Y-(1/2)|\zeta|}^{Y+(1/2)|\zeta|}\frac{d\eta}{2Y}R_2(\eta,\zeta)\ . \tag{2.16}$$

$\bar{R}_2$ has a ζ dependence through the finite integration domain as well as the intrinsic ζ dependence of R_2. Only if the correlation length ξ is substantially less than Y does this really improve the situation. For example, we need, for overall translational invariance, $\sigma\ll Y$ and for the factorization of variables in Eq. (2.16) $Y\ll\zeta$, $\xi\ll\sigma$. These conditions give $\xi\ll Y\ll\sigma$ which yields, in Eq. (2.14),

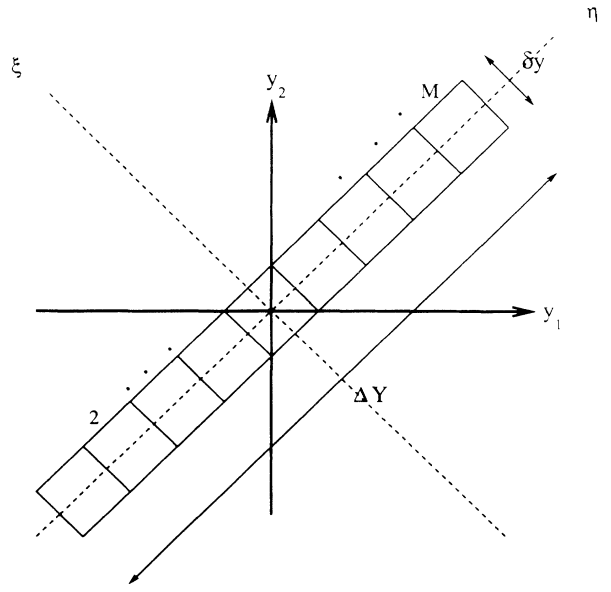

FIG. 2. The integration domain in the c.m. and relative variables is shown.

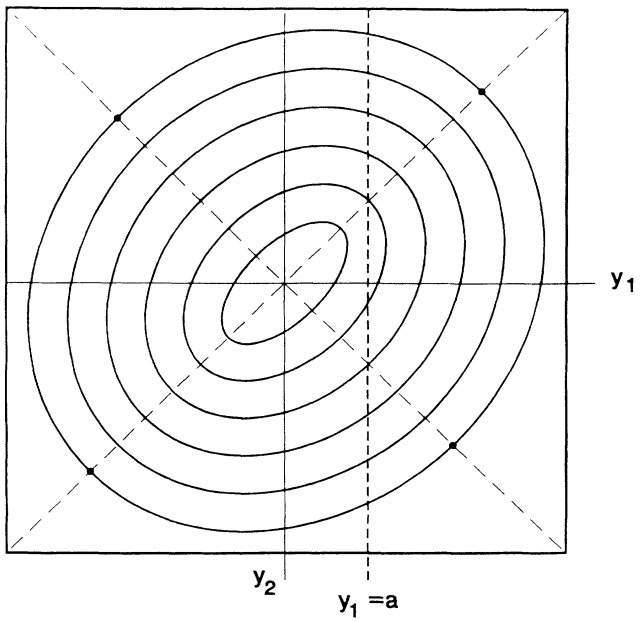

FIG. 3. Contour map of the $R_2(y_1,y_2)$ in Eq. (2.10).

$$\bar{R}_2(Y,\xi) \simeq \int_{-Y}^{Y} \frac{d\eta}{2Y} R_2(\eta,\xi) ,$$
$$\Gamma(q,Y) \simeq \int_{-Y}^{Y} d\xi \, \bar{R}_2(Y,\xi) e^{-iq\xi} . \tag{2.17}$$

In the example of (2.14) the effect of nonstationary only shows up as a multiplicative constant. The contour plot of Fig. 3 now becomes a narrow mountain of small width 2ξ.

Most experimental data are presented not as contour plots such as Fig. 3, but as plots of y_2 for fixed y_1. This corresponds to a vertical cut in Fig. 3, thereby inducing asymmetries not present when η and ξ are used. The example (2.14) shows that R_2 may simply factor when expressed in these variables, i.e., the dependence on ξ is multiplied by an envelope function depending on η. In many cases of interest we do not need strict inequalities (such as $\xi \ll Y$) nor can we expect them. The best procedure is to inspect the correlation data numerically to see whether Eq. (2.13) is a decent approximation. To be sure, Eq. (2.9) is exact, but its physical interpretation is a bit obscure. We also note that since $\Gamma(q,Y)$ depends only on one variable q, we cannot express $R_2(y_1,y_2)$ in terms of it by an inverse Fourier transform, thereby losing the essence of the Wiener-Khinchin theorem. It is not clear that there is any merit in considering such objects as $\langle \hat{r}_q \hat{r}^*_{q'} \rangle$ whose precise knowledge would allow a double-Fourier inversion in principle, but probably not in practice.

The following argument is frequently used to motivate the equivalence of ensemble and time averages for correlation functions. From a long time signal one cuts pieces of length $2T$ such that there are many samples of this length, which comprise the members of the equivalent ensemble. We could imagine constructing a long pseudostationary rapidity signal by adjoining independent $\hat{r}(y)$ measurements of length $2Y$ (see Fig. 4). Clearly this will not allow correlations between $Y-\epsilon$ and $Y+\epsilon$, for example. In fact the ability to ignore correlations between adjacent time intervals $2T$ is necessary for the validity of the argument of the equivalence of ensemble and time series (e.g., ergodic limit). However, using the pseudostationary signal $\hat{r}_{ps}$ of Fig. 4 alleviates integration domain problems as shown in Fig. 2. For this process the modified power spectrum is

$$\Gamma(q) = \lim_{p\to\infty} \frac{\langle :|\hat{r}_{ps}(q,s)|^2: \rangle}{2pY} = \lim_{p\to\infty} \frac{1}{2pY} \int_{-pY}^{pY} dy_1 \int_{-pY}^{pY} dy_2 \langle :\hat{r}_{ps}(y_1,s)\hat{r}_{ps}(y_2,s): \rangle . \tag{2.18}$$

In Fig. 2 the point marked A describes $y_1 = \delta y + \epsilon$ in the second bin, close to the point $y_2 = \delta y - \epsilon$ in the fundamental bin. We expect such correlations to be small in a large ensemble. In this way a quasistationary rapidity signal is constructed. By choosing random assignments of separate event traces in sequential intervals one can test the validity of this hypothesis.

As is clear from (2.17), the class of quasistationary correlations shares the simplicity of truly stationary processes. In particular we can compute the correlation function $R_2(\xi)$ from the experimentally determined $\Gamma(q)$, i.e., from Eq. (2.8).

Prototypical examples are given in Table I ($p \to \infty$).

III. GENERALIZATION TO SUBSPACES: FOURIER INTERMITTENCY ANALYSIS

For clarity the analysis of Sec. II was done for the full rapidity interval $-Y < y < Y$. Clearly variants of this choice are possible and even desirable. For instance, one can choose $2Y$ to be a smaller interval over which rapidity density is essentially stationary. For this to be useful 2ξ must be less than $2Y$, if we are to attempt a calculation of the correlation function from the power spectrum. From the discussion at the end of the Appendix, we observe that for broad mixed-multiplicity distributions, all the effects under discussion may be dominated by single-particle density "fluctuations" [see Eqs. (A7) and (A8)] and possibly be of little intrinsic interest.

In the bin-averaging technique of Białas and Peschanski [6], one subdivides the interval $2Y$ into M equal bins of width $\delta y = 2Y/M$. Integration of the two-particle density correlations over bin i gives ($\bar{\rho}_i$ is the average density in bin i)

$$\frac{1}{(\delta y)^2} \int_{\Omega_i} \int \frac{\rho_2(y_1,y_2)dy_1 dy_2}{(\bar{\rho}_i)^2} = \frac{\langle n_i(n_i-1) \rangle}{\langle n_i \rangle^2} , \tag{3.1}$$

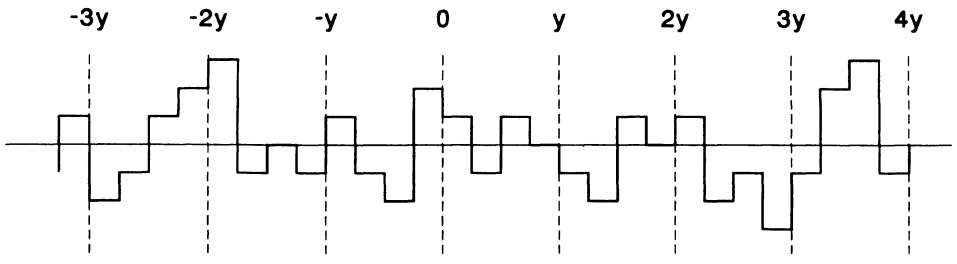

FIG. 4. Construction of a event ensemble from a long time series.

TABLE I. Various time signals and their power spectra.

Time signal	$\Gamma(q)\propto$
1. White noise	Constant
2. Periodic	$\delta q, q_1+\delta q, -q_1$
3. Exponential	$(q^2+\xi^2)^{-1}$
4. Scaling	$q^{1-D}, 0<d<1$
5. Chaotic	Special analysis

where Ω_i denotes an integration domain where y_1, y_2 run over the same interval of length δy. [Equation (3.1) can be compared with Eq. (2.5), which gives the corresponding result for the second-order cumulant.] Bin averaging now gives, in pth order,

$$F_p(\delta y)=\frac{1}{M}\sum_{i=1}^{N}\frac{1}{(\delta y)^p}\int_{\Omega_i}\int dy_1\cdots dy_p\frac{\rho_p(y_1\cdots y_p)}{(\bar{\rho}_i)^p}\ . \tag{3.2}$$

In Fig. 2 the hatched squares correspond to the integration domains of individual bins. In practice one increases M as much as possible in order to test the δy dependence of F_p. It is also useful to define bin-averaged factorial cumulants K_p in terms of the cumulant correlation functions, as discussed in Ref. [18], since the new correlation information expressed in successive order is contained in the highest cumulant.

We can now write a "bin-averaged" power spectrum as

$$K_2(q,\delta y)=\frac{1}{M(\delta y)^2}\sum_{i=1}^{M}\int_{\Omega_i}dy_1\int_{\Omega_i}dy_2\frac{C_2(y_1,y_2)}{(\bar{\rho}_i)^2)}\times e^{iq(y_2-y_1)}\ , \tag{3.3}$$

$$F_2(q,\delta y)=\frac{1}{M(\delta y)^2}\sum_{i=1}^{M}\int_{\Omega_i}dy_1\int_{\Omega_i}dy_2\frac{\rho_2(y_1,y_2)}{(\bar{\rho}_1)^2}\times e^{iq(y_2-y_1)} \tag{3.4}$$

for the reduced cumulant $R_2=C_2/(\bar{\rho}_2)^2$ and reduced density $r_2=\rho_2(y_1,y_2)/(\bar{\rho}_1)^2$. (The advantages of the local normalization to $\bar{\rho}_1$ for the bin analysis was explained in Ref. [18].)

If M becomes large the fraction of the joint phase space $-Y<y_1,y_2<Y$ used in the integrations (3.2)–(3.4) is $1/M$. If $q\delta y\ll 1$, Eqs. (3.3) and (3.4) reduce to the usual moments [see Eq. (3.2)]. Hence we need Fourier coefficients of wave vector q having harmonic number n satisfying $n\gtrsim M/\pi$ to see an effect. For example, if $M=20$, the first six harmonics do not cause the generalized moments to deviate from $F(0,\delta y)$. One then has to look at higher-frequency componets as $\delta y\to 0$ for fluctuations. Hence the practical utility of (3.3) and (3.4) may be doubted.

For large M, the bin integration domain is well approximated by the strip (see Fig. 2). For translation-invariant correlations this greatly simplifies back-of-the-envelope calculations. Alternatively we can define a different type of moment which is exact in the strip domain. This is not to be regarded as an approximation to the bin moments, but as a different construction of equal merit. Note that since $\hat{\rho}_2$ just counts points, the strip integral gives [see Eq. (2.1)]

$$\int_{\text{strip}}dy_1\,dy_2\,\hat{\rho}_2(y_1,y_2;\mathbf{s})=\sum_{i\neq j}\theta(\delta y/2-|s_i-s_j|)\ , \tag{3.5}$$

where θ is unity for positive arguments and zero otherwise. The strip integration has the same area as the unrotated rectangular counterpart. Note that (3.5) simply counts the number of pairs of points in the strip whose separation is less than δy. Note further that we did not use an ensemble average, or say anything about translational invariance. This formula has been much used to study fractals generated by time series of maps in chaotic domains [20,21].

Before analyzing (3.5) further we give a simple example, averaging uniformly over the η direction for the c.m. variables $(s_i+s_j)/2$. Dividing the integrand in (3.5) by $M\delta y^2\bar{\rho}_1^2$ we define the analogies of F_2 given in Eq. (3.2) and $F_2(q,\delta y)$ similar to Eq. (3.4):

$$F_2(\delta y)\equiv\frac{1}{\delta y}\int_{-\delta y/2}^{\delta y/2}d\xi\frac{\rho_2(\xi)}{\rho_1^2}\ ,$$
$$F_2(q,\delta y)\equiv\frac{1}{\delta y}\int_{-\delta y/2}^{\delta y/2}d\xi\frac{\rho_2(\xi)e^{-iq\xi}}{\rho_1^2}\ . \tag{3.6}$$

In order to illustrate the effect of introducing the Fourier transform generalization we carry out an analytic evaluation using a standard exponential fit to the cumulant R_2:

$$R_2(\xi)=\frac{\rho_2(\xi)}{\rho_1^2}-1=\gamma\exp(-|\xi|/\xi)\ . \tag{3.7}$$

Equations (3.6) now give

$$F_2(x)=1+\frac{\gamma}{x}(1-e^{-x})\ ,$$
$$F_2(x,y)=1+\frac{\gamma}{x}\frac{1-e^{-x}(\cos xy-y\sin xy)]}{1+y^2}\ , \tag{3.8}$$
$$x\equiv\frac{\delta y}{2\xi},\quad y=q\xi\ .$$

By fitting $F_2(\delta y)$ to existing NA22 data we found $\gamma=0.4$, $\xi=1.35$ to give a good description of experimental results [4].

It is easy to confirm that as $x\to 0$ both expressions in Eq. (3.8) tend to limit

$$F_2(x)\sim F_2(x,y)\sim\gamma+1,\ x\to 0\ . \tag{3.9}$$

For large x, we find

$$\frac{F_2(x,y)-1}{\gamma}\to\frac{1}{1+y^2},\quad x\to\infty\ . \tag{3.10}$$

Clearly the most interesting feature of the Fourier generalization is the modification—with possible oscillations—of the usual moment. The decisive scale here is the correlation "length" ξ, in terms of which $\delta y(\to x)$ and $q(\to y)$ are measured. Figure 5 shows the behavior of $K_2(x,y)$ (defined to be $[F_2(x,y)-1]/\gamma$ as in (3.10)) for various values of $y=q\xi$. The oscillations in-

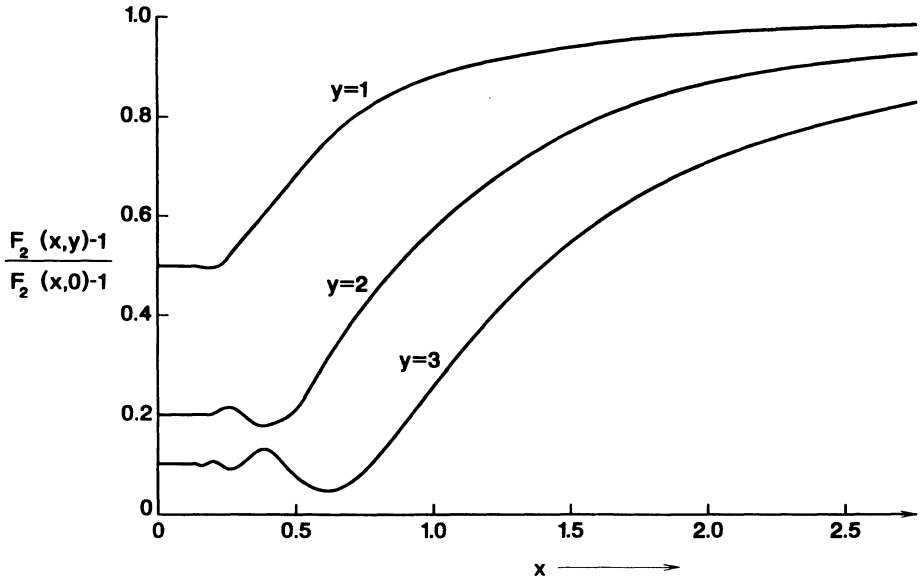

FIG. 5. The ratio $[F_2(x,y)-1]/[F_2(x,0)-1]$ of cumulant-type moments is shown as a function of x for $y=q$, $\zeta=1$, 2, and 3. The oscillations increases with increasing y and decreasing x but are damped by the combination η, the exponential, and the $(1+y^2)$ demoninator of Eq. (3.8).

duced into the factorial moments by the Fourier probe clearly provide much greater detail about the correlation function than can be obtained from the usual moments. Although the principal recent interest has been for small bin width, this method is most accessible for larger bin width, since it is easier to assess real data for the larger δy values. We notice that, in principle, it is possible to construct the correlation function $\rho_2(\zeta)$ from $F_2(q,\delta y)$ by inverse Fourier transform, an act not possible in the usual bin-averaged factorial moment approach.

We now turn to Eq. (3.5). The simplest way to prove the result is to change variables $y_1 y_2 \to \eta,\zeta$ and analogously for the pairs s_i,s_j. Equation (2.1) can be written as

$$\hat{\rho}_2(\eta,\zeta;\mathbf{s})=\sum_{i\neq j}\delta\left[\eta-\frac{s_i+s_j}{2}\right]\delta(\zeta-(s_j-s_i)) . \tag{3.11}$$

The strip integration gives unity for each pair whose separation is less than δy and whose c.m. lies in the length $(2Y)$ of the strip. This is also the content of Eq. (2.5). Note that if we assume factorization of the pair probabilities

$$P(s_i,s_j)=P\left[\frac{s_i+s_j}{2}\right]P(s_i-s_j) , \tag{3.12}$$

the ensemble average reduces to

$$\int_{\text{strip}}\rho_2(\eta,\zeta)d\eta\,d\zeta=\sum_{i\neq j}\langle\theta(\delta y/2-|s_j-s_i|)\rangle . \tag{3.13}$$

Equation (3.12) is more general than translation invariance. Actually for narrow strips $\delta y \ll Y$ is automatically satisfied; hence, (3.12) becomes unnecessary.

Slipping a factor $\exp(-iq\zeta)$ in the integral (3.13) we find

$$\int_{\text{strip}}\rho_2(y,\zeta)e^{-iq\zeta}dy\,d\zeta=\sum_{i\neq j}\langle e^{iq(s_j-s_i)}\theta(\delta y/2-|s_j-s_i|)\rangle . \tag{3.14}$$

Recalling the definition of ρ_q [see Eq. (2.7)], the right-hand side of (3.14) can be written as

$$\langle\langle\hat{\rho}_q^*(\mathbf{s})\hat{\rho}_q(\mathbf{s})\rangle\rangle-\langle n\rangle , \tag{3.15}$$

where the double angular brackets enforce the restriction $|s_i-s_j|<\delta y$ and $i\neq j$. Note that (3.15) is a familiar object appearing in the interaction energy of a many-particle system with potential energy $\sum_{i<j}v_{ij}$:

$$\langle V\rangle=\tfrac{1}{2}\int_{\text{strip}}dx_1\,dx_2\,\rho_2(x_1,x_2)v(x_1-x_2)=\sum_q v(q)[\langle\langle\hat{\rho}_q^*\hat{\rho}_q\rangle\rangle-\langle n\rangle] . \tag{3.16}$$

The absence of translational invariance, if any, survives purely in the distribution of points s_i, whose relative distance is all that matters in Eqs. (3.13) and (3.14).

We note that Eq. (3.5) is ordinarily used for the $n\to\infty$ limit of a time series inhabiting a finite time interval. In this way a dense distribution of points is built up in a way conceptually different from, but not necessarily in disagreement with, the viewpoint of Eq. (1.3).

Equation (3.13) allows the computation of $\rho_2^{(n)}(\zeta)$ once the right-hand side is known. But note that, in contrast with expressions such as Eqs. (2.8)–(2.13), much more computation is required. For the latter we simply square $\hat{r}_q$ (or $\hat{\rho}_q$, determined by summing over n coordinates (and then perhaps averaging over n.) But for the computation of $\langle\rho_q^*(\mathbf{s})\rho_q(\mathbf{s})\rangle$ we must assure that the $n(n-1)$ conditions $|s_i-s_j|<\epsilon$ are met. Hence the cost of the generalization of the Wiener-Khinchin theorem to nontranslation-invariant cases by this method is accom-

plished at the cost of increased computational complexity.

By construction, Eqs. (3.12)–(3.14) are insensitive to the "local" structure of the set as measured by $(s_i+s_j)/2$. This situation is complementary to the technique of the Wigner transform [22]

$$F(q,Y)=\int d\xi\, e^{-iq\xi}\langle\hat{\rho}(Y-\tfrac{1}{2}\xi)\hat{\rho}(Y+\tfrac{1}{2}\xi)\rangle\ . \quad (3.17)$$

This function satisfies the identities

$$\int\frac{dq}{2\pi}F(q,Y)=\langle|\hat{\rho}(y)|^2\rangle\ ,$$
$$\int dY\,F(q,Y)=\langle|\hat{\rho}_q|^2\rangle\ . \quad (3.18)$$

Another technique recently developed to study the local texture of distributions is the "wavelet" transform [23]. We shall not pursue this technique here.

IV. CHAOTIC EXAMPLE OF THE POWER SPECTRUM

In this section we use one-dimensional discrete maps to generate power spectra in different dynamical regimes. Recently such structures have been studied [17] in the context of factorial moments and cumulants in order to make comparisons with the experimental observations of hadronic rapidity correlations. The characterization of dynamically different regimes in those models is essential in distinguishing the contributions from chaotic and deterministic components. For this characterization, the factorial-moment method is complemented by the study of multifractal structures and the power spectrum of the rapidity distribution. In fact the importance of the power-spectrum analysis was emphasized much earlier [13] than the factorial-moment approach. We are not aware of any published power-spectrum analysis of the available data on hadron collisions since then. In Ref. [13] a smooth rapidity distribution generated from an experimental rapidity histogram by a Monte Carlo simulation averaged over an experimentally reasonable number of events was produced to yield a structureless event-averaged power spectrum. A systematic accumulation of peaks at low frequencies was observed when each individual event was superimposed on the numerically simulated smooth event-averaged power spectrum: this was suggested as an indication of nonstatistical fluctuations in the rapidity distributions. We suggest here that this method may not be sufficiently accurate to see the existence of a nontrivial dynamics. This can be checked directly in one-dimensional maps by tuning the strength of the nonlinearity. In Fig. 6 we present a simulated power spectrum for 1000 events with 200 particles per event using the tent map in the fully chaotic (Gaussian) regime. Each event is generated by iterating the map to produce particles at rapidity points y_j where $(j=1,\ldots,200)$ starting from a uniformly random initial value. Instead of studying the power spectrum of the rapidity density $\hat{\rho}(y)$ we investigate the fluctuations from the event-averaged rapidity density $\langle\rho_1(y)\rangle$ as follows:

$$C_2(q)=|\hat{\rho}_q|^2-|\langle\hat{\rho}_q\rangle|^2\ , \quad (4.1)$$

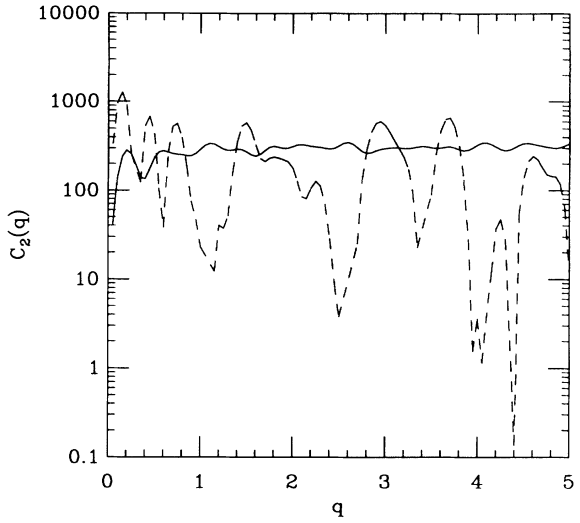

FIG. 6. Power spectrum of the Gaussian white noise generated by the tent map $[x_{n+1}=2\lambda(0.5-|x_n|);\ 0\geq|x|\geq 0.5]$ in the fully chaotic regime. Solid line is the event average and the dotted line is a particular event.

where the power spectrum $\hat{\rho}_q$ of the one-dimensional map is calculated using Eqs. (2.7) and (2.8). Equation (4.1) refers to the deviation in the power spectrum of a particular event from the average. The event-averaged fluctuation $\langle C_2(q)\rangle$ is given by averaging (4.1) over all events.

As was shown in Ref. [17], the fully chaotic tent map provides a good representative of the Gaussian white noise. This is also confirmed by the smoothness of the power spectrum on a logarithmic scale as shown in Fig. 6. We have superimposed the power spectrum of a particular event on the event-averaged power spectrum of this Gaussian model. Large deviations from the event seem to indicate the presence of nonrandom structures; however, these fluctuations do not show any coherence from one event to the other. Therefore, deviations from the average power spectrum are totally statistical in origin. In order to show that, if they exist, dynamical (nonstatistical) fluctuations should survive the event average of the power spectrum, we have studied the logistic map [17] in the non-Gaussian intermittent regime.

The fluctuations in this non-Gaussian model as shown in Fig. 7 survive the event averaging, implying that the fluctuations are dynamical in origin. The power spectrum $C_2(q)$ of an arbitrary event follows an identical pattern to the event-averaged $\langle C_2(q)\rangle$ in all frequency domains.

A close look at both figures indicates that in Fig. 7, event-to-event dynamical fluctuations of the power spectrum interfere coherently; as a result of this, the event average is indistinguishable from an arbitrary event.

Factorial-moment analysis in the rapidity space often encounters the problem of minimum biasing which is essentially nothing but aligning the central rapidity of each event histogram such that minimum statistical fluctuations are observed in the average process. Power-spectrum analysis, on the other hand, is canonical to the factorial-moment technique since it is performed in the

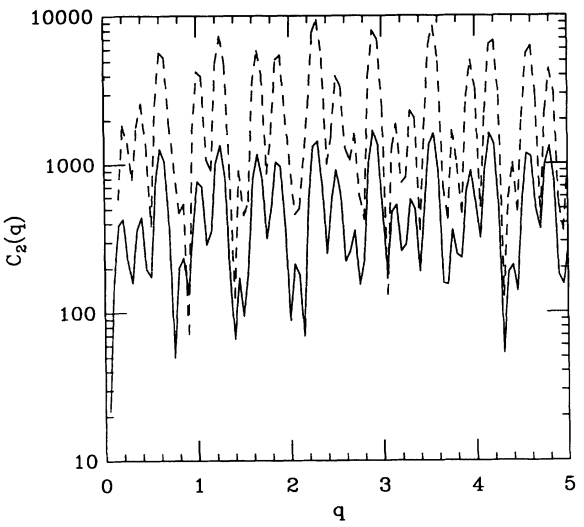

FIG. 7. Power spectrum of the non-Gaussian logistic map $[x_{n+1}=\lambda x_n(1-x_n)]$ in the intermittent regime ($\lambda=3.83$). The solid line is the event average and the dotted line is a particular event.

boost space. In this respect the latter technique avoids the problems of centralization.

Let us consider an observable $y(t)$ that is generated by a dynamical law:

$$y(t+1)=F[y(t)] . \tag{4.2}$$

We can generate different events from $y(t)$ by uniformly reshuffling the rapidity histograms. For instance a mapping $f(t)$ can be defined which has a chaotic distribution such that $y(f(t))$ is considered as a different event. The mapping $f(t)$ is chosen such that it is uniform and preserves the phase-space volume. With these conditions, the dynamical fluctuations present in (4.2) remain intact. This last statement is identical to saying that the hierarchy of correlation functions $C_p(t_1,t_2,\ldots,t_p)$ describing the underlying dynamics are unchanged by $t_i\to f(t_i)$ $(i=1,\ldots,p)$. If $y(t)$ itself is a Gaussian white noise,

$$\langle y(t)y(t')\rangle \propto \delta(t-t') . \tag{4.3}$$

We notice that (4.3) also means that no correlations exist between different events:

$$\langle y(t)y(f(t))\rangle \propto \delta(t-f(t))=0 \tag{4.4}$$

since $f(t)$, by it's chaotic construction, is not allowed to have fixed points.

On the other hand, if $y(t)$ has nontrivial internal correlations,

$$\langle y(t)y(t')\rangle \propto G(t,t') . \tag{4.5}$$

In general $G(t,t')$ is not translationally invariant or in a broader perspective, factorization of pair probabilities as in Eq. (3.12) may not be true. As a result of this, correlations between different events generated by the chaotic uniform reshuffling are nonvanishing:

$$\langle y(t)(f(t))\rangle \propto G(t,f(t))\neq 0 . \tag{4.6}$$

Namely, in the presence of fully intermittent dynamical correlations, different events may look correlated which is also confirmed in the numerical example of Fig. 7.

In short a simple power-spectrum analysis of the rapidity density reveals the qualitative features of the fluctuations. We suggest that the event-averaged power spectrum itself should retain the properties of nontrivial dynamics as opposed to fluctuations of a particular event from the average as studied in Ref. [13].

V. DISCUSSION AND SUMMARY

Idealistically the probabilities p_n and $Q_n(s_1,s_2,\ldots,s_n)$, although used classically (as is appropriate), are properly derived from the S matrix for the n-particle reaction. The sequence of correlation functions under investigation, and the probability counts for various parts of phase space, provide constraints on the statistical-dynamical properties of the underlying theory. For example, negative-binomial counts, together with the linked-pair structure of higher-cumulant correlation functions, represent a fascinating regularity in multiplicity distributions induced by hadron-hadron collisions as well as in galaxy distributions.

In Ref. [14] we reviewed the natural kinematical origin of the rapidity variable. It is of great interest that this variable has an operator form naturally connected to the algebra of the Poincaré group [24]. Denoting the energy-momentum tensor by $\theta_{\mu\nu}$ we have

$$\begin{aligned} &Y_{\rm op}\equiv\frac{1}{2}\ln\frac{H+P_z}{H-P_z} , \\ &H=\int\theta_{00}d^3x, \quad P_z=\int\theta^{0z}d^3x , \\ &K_z=t\int\theta^{0z}d^3x+\int z\theta_{00}d^3x . \end{aligned} \tag{5.1}$$

The spectrum of $Y_{\rm op}$ and the Lorentz-boost operator K_z are continuous and range from $-\infty$ to $+\infty$. Rapidity is canonical to boosts as shown by

$$[Y_{\rm op},K_z]=i . \tag{5.2}$$

Hence the Fourier-transform variable q used throughout this paper is to be identified with the boost eigenvalue. In this way the noncompact nature of kinematical properties of group representations of the S matrix may be of use.

Next we review the main results of this paper. In Sec. II we analyzed modifications of the usual power-spectrum analysis required by the finite rapidity interval and the nonstationary character of the rapidity density and the correlation function. We noted that the cumulant correlations, normalized to the appropriate single-particle rapidity densities, gave rise to bin-independent relative fluctuations when the empirically successful negative-binomial distribution is used. We then expressed the power spectrum in terms of an integral over a two-dimensional rapidity phase space. Although it is impossible to recover the full correlation function from this general expression, we defined an average [over the c.m. vari-

able $(y_1+y_2)/2]$ correlation function $\bar{R}_2(\zeta)$ that seems appropriate to the actual quasistationary situation. In Sec. III the ideas inherent in the Wiener-Khinchin theorem were used to generalize the bin-averaged factorial and factorial moment and cumulant methods. Still more interesting is the discovery that the corresponding generalization of the "strip" integral of the two-particle correlation function yields an expression which depends on the relative coordinates even when the underlying distribution is not stationary. In the limit $q\to 0$ the Grassberger-Procaccia method [20] for computing the correlation dimension is recovered. In Sec. IV we studied the power spectra and correlation functions of "data" generated by finite samples of a chaotic time series. We numerically verified distinct properties of the power spectrum in two cases of statistically and dynamically generated fluctuations. In the Appendix we give the recipe for the evaluation of generalized power spectra for higher-order correlations from two points of view: (1) the linked-pair approximation and (2) the simple form of cumulants of single-particle density fluctuations.

ACKNOWLEDGMENTS

This research was supported in part by the U.S. Department of Energy Divisions of High Energy and Nuclear Physics. One of the authors (P.C.) is indebted to the Alexander von Humboldt Foundation, and to the Gesellschaft für Schwerionenforschung (Darmstadt) and Professor W. Greiner of the J. W. von Goethe University, Frankfurt am Main, Institute for Theoretical Physics for hospitality during the completion of this work.

APPENDIX: POWER SPECTRA OF HIGHER-ORDER CORRELATIONS

Consider the reduced third- and fourth-order cumulant correlations functions

$$k_3(y_1,y_2,y_3)\equiv\frac{C_3(y_1,y_2,y_3)}{\rho_1(y_1)\rho_1(y_2)\rho_1(y_3)}=\langle\hat{r}(y_1)\hat{r}(y_2)\hat{r}(y_3)\rangle\ , \tag{A1}$$

$$\begin{aligned}k_4(y_1,y_2,y_3,y_4)&\equiv\frac{C_4(y_1,y_2,y_3,y_4)}{\rho_1(y_1)\rho_1(y_2)\rho_1(y_3)\rho_1(y_4)}\\&=\langle\hat{r}(y_1)\hat{r}(y_2)\hat{r}(y_3)\hat{r}(y_4)\rangle\\&\quad-\sum_{\text{perms}}\langle\hat{r}(y_1)\hat{r}(y_2)\rangle\langle\hat{r}(y_3)\hat{r}(y_4)\rangle\ .\end{aligned}$$

It is understood that overlapping arguments are to be excluded for systems composed of one species of particles. This counting convention is equivalent to normal ordering of creation and destruction operators for the corresponding number densities.

Previously we proposed a numerically successful [4,18] composition formula for the reduced cumulants [the linked-pair approximation (LPA)]:

$$\begin{aligned}k_3(1,2,3)&=\frac{A_3}{3}[k_2(1,2)k_2(2,3)+k_2(2,3)k_2(3,1)\\&\quad+k_3(3,1)k_2(1,2)]\ ,\\k_4(1,2,3,4)&=\frac{A_4}{12}\sum_{\text{perms}}k_2(1,2)k_2(2,3)k_2(3,4)\ .\end{aligned} \tag{A2}$$

In the case of translation invariance the integration over all dy_i in a strip $-\delta y/2<\zeta_{ij}<\delta y/2$, $-Y/2<\eta<Y/2$ gives $A_p k^{-p+1}$ for a negative-binomial distribution with $1/k$ given by the integral of Eq. (2.5). In pth order the natural variables are $Y=(y_1+y_2+\cdots+y_p)/p$ and $p-1$ of the relative coordinates $\zeta_{ij}=y_j-y_i$. (For comparison of the strip and bin integrations domains see Ref. [11].) The values $A_p=(p-1)!$, which lead to negative-binomial counting distributions, are suggested by empirical fits to the hadronic data [3,18].

Unlike the exposition of Eqs. (2.1)–(2.13), it is not simple to integrate out the c.m. variable. For quasistationary examples of Sec. II the overall c.m. dependence can be shown here also to factor out; hence, the LPA coefficients A_p become Y dependent. Here we only state the results for transition invariance:

$$\begin{aligned}&\int dy_1\,dy_2\,dy_3\exp\left[i\sum q_i y_i\right]k_3(y_1,y_2,y_3)\\&\quad=\frac{A_3\Delta Y}{3}[k_2(q_1)k_2(q_2)+k_2(q_2)k_2(q_3)\\&\qquad+k_2(q_3)k_2(q_1)]\ ,\end{aligned} \tag{A3}$$

where $q_1+q_2+q_3=0$ as a consequence of translation invariance. Clearly this structure extends to higher orders: $\sum_{j=1}^{p}q_j=0$ and the p-dimensional Fourier transform of k_p is the symmetrized product of $p-1$ distinct two-particle power spectra $k_2(q)$. Hence in the LPA the generalized power spectrum of the pth cumulant correlation function is expressible in terms of products of power spectra of the two-particle correlation function.

Since the linked-pair (hierarchical) formulas are apparently valid for coarse-grained galaxy distributions [19] which are approximately translation invariant, they may be of greater utility for astronomy than particle physics. In any case it is hard to get detailed information about the correlation functions of order three and higher, even though the factorial moments (the averaged correlation functions) can be measured.

Although the expressions (A2) seem to work, there is as yet no dynamical explanation for their origin, either in strong interactions or in cosmology. Therefore, another set of relations, of greater use for broad count distributions, is of interest. As mentioned before, measured correlation functions involve mixtures of differing multiplicities [see Eq. (2.3)]. If we define general and fixed n second-order cumulants by

$$\begin{aligned}C_2(y_1,y_2)&=\rho_2(y_1,y_2)-\rho_1(y_1)\rho_1(y_2)\ ,\\C_2^{(n)}(y_1,y_2)&=\rho_2^{(n)}(y_1,y_2)-\rho_1^{(n)}(y_1)\rho_1^{(n)}(y_2)\ ,\end{aligned} \tag{A4}$$

one finds the connection

$$C_2(y_1,y_2)=\langle C_2^{(n)}(y_1,y_2)\rangle+\langle \Delta\rho_n(y_1)\Delta\rho_n(y_2)\rangle \ , \tag{A5}$$

where the angular brackets are an average over p_n [see Eq. (1.3)] and $\Delta\rho_n$:

$$\Delta\rho_n(y)=\rho_1^{(n)}-\rho_1(y) \tag{A6}$$

is the single-particle density fluctuation due to the fluctuating multiplicity. This decomposition can be extended to higher orders [2], for example,

$$\begin{aligned} C_3(y_1,y_2,y_3)=&\langle C_3^{(n)}(y_1,y_2,y_3)\rangle \\ &+\sum_{\text{perms}}\langle \Delta C_2^{(n)}(y_1,y_2)\Delta\rho_n(y_3)\rangle \\ &+\langle \Delta\rho_n(y_1)\Delta\rho_n(y_2)\Delta\rho_n(y_3)\rangle \end{aligned} \tag{A7}$$

with $\Delta C_2^{(n)}=C_2^{(n)}-C_2$. Since the integrals of the correlation functions obey sum rules (connecting them to the ordinary moments), one can estimate the numerical importance of the various contributions to (A5)–(A7). In particular the pure $\Delta\rho$ terms give rise to ordinary cumulant moments, while the left-hand side C_p gives factorial cumulant moments. The integral versions of (A5) and (A7) are

$$\begin{aligned} \frac{f_2}{\langle n\rangle^2}&=-\frac{1}{\langle n\rangle}+\gamma_2 \ , \\ \frac{f_3}{\langle n\rangle^3}&=\frac{2}{\langle n\rangle^2}-\frac{3}{\langle n\rangle}\gamma_2+\gamma_3 \ , \end{aligned} \tag{A8}$$

where

$$\begin{aligned} \gamma_2&=\langle (n-\langle n\rangle)^2\rangle/\langle n\rangle^2,\ldots, \\ \gamma_3&=\langle (n-\langle n\rangle)^3\rangle/\langle n\rangle^3,\ldots \ . \end{aligned}$$

For broad distributions such as the negative binomial, $\gamma_p=O(\langle n\rangle^0)$ and the last term dominates. Therefore, we can conclude that the dominant contribution to the factorial-cumulant correlation function C_p comes from the single-particle density fluctuation term. The detailed dynamics contained in fixed n correlation functions is therefore negligible with regard to mixed N for such situations.

In this case we have

$$\begin{aligned} C_2&\sim\langle \Delta\rho_n(1)\Delta\rho_n(2)\rangle \ , \\ C_3&\sim\langle \Delta\rho_n(1)\Delta\rho_n(2)\Delta\rho_n(3)\rangle \ , \\ C_4&\sim\langle \Delta\rho_1(1)\Delta\rho_n(2)\Delta\rho_n(3)\Delta\rho_n(4)\rangle \\ &\quad-\sum_{\text{perms}}\langle \Delta\rho_n(1)\Delta\rho_n(2)\rangle\langle \Delta\rho_n(3)\Delta\rho_n(4)\rangle \ , \end{aligned} \tag{A9}$$

i.e., the single-particle density cumulants. Corresponding to Eq. (A9) we write

$$\begin{aligned} k_2&=\frac{C_2}{\rho_1(1)\rho_1(2)}\sim\langle r_n(1)r_n(2)\rangle \ , \\ k_3&=\frac{C_3}{\rho_1(1)\rho_1(2)\rho_1(3)}\sim\langle r_n(1)r_n(2)r_n(3)\rangle \ , \\ k_4&=\frac{C_4}{\rho_1(1)\rho_1(2)\rho_1(3)\rho_1(4)} \\ &\sim\langle r_n(1)r_n(2)r_n(3)r_n(4)\rangle \\ &\quad-\sum_{\text{perms}}\langle r_n(1)r_n(2)\rangle\langle r_n(3)r_n(4)\rangle \ , \end{aligned} \tag{A10}$$

with r_n defined as [compare with Eq. (1.4)]

$$r_n(y)=(\rho_n(y)-\rho(y))/\rho(y) \ . \tag{A11}$$

We can imitate (2.14) as follows:

$$\begin{aligned} \tilde{\Gamma}_2(q)&=\lim_{p\to\infty}\frac{\langle |r_n(q)|^2\rangle}{2pY} \\ &=\sum_n p_n\Gamma_2^{(n)}(q) \\ &=\lim_{p\to\infty}\frac{1}{2pY}\int_{-Y}^{Y}dy_1\int_{-Y}^{Y}dy_2\,e^{iq(y_1-y_2)}k_2(y_1,y_2) \ . \end{aligned} \tag{A12}$$

For higher orders we obtain, for example,

$$\begin{aligned} \tilde{\Gamma}_3(q_1,q_2,q_3)&=\lim_{p\to\infty}\frac{\langle r_n(q_1)r_n(q_2)r_n(q_3)\rangle}{2pY}\delta_{q_1+q_2+q_3,0} \\ &=\lim_{p\to\infty}\frac{1}{2pY}\int dy_1\,dy_2\,dy_3\,e^{iq_1y_1+q_2y_2+q_3y_3}k_3(y_1,y_2,y_3) \ . \end{aligned} \tag{A13}$$

In Eq. (A12) we see that the Fourier transform of k_2 is given in terms of the single-particle density fluctuation $r_n(q)$ averaged over the probability distribution p_n.

[1] P. Carruthers, Int. J. Mod. Phys. A **4**, 5587 (1989).

[2] P. Carruthers, Phys. Rev. A **43**, 2632 (1991).

[3] P. Carruthers, in *Proceedings of the Marburg Workshop on Correlations and Multiparticle Production*, Marburg, Germany, 1990, edited by M. Plümer, S. Raha, and R. M. Weiner (World Scientific, Singapore, 1991), p. 369.

[4] P. Carruthers and I. Sarcevic, Phys. Rev. Lett. **63**, 1562 (1989).

[5] A. Capella, K. Fialkowski, and A. Krzywicki, Phys. Lett. B **230**, 149 (1989).

[6] A. Bialas and R. Peschanski, Nucl. Phys. **B273**, 703 (1986); **B308**, 857 (1988).

[7] W. Kittel and R. Peschanski, in *Proceedings of the International Europhysics Conference on High Energy Physics,*

Madrid, Spain, 1989, edited by F. Barreiro and C. Lopez [Nucl. Phys. B (Proc. Suppl.) **16**, 445 (1990)].

[8] A. Giovannini, Nuovo Cimento **15A**, 543 (1973).

[9] P. Carruthers and Ming Duong-Van, Los Alamos Report No. LA-UR-83-2419 (unpublished).

[10] P. Carruthers, *Multiparticle Production,* in Proceedings of the Perugia Workshop, Perugia, Italy, 1988, edited by R. Hwa, G. Pancheri, and Y. Srivastava (World Scientific, Singapore, 1989), p. 190; in *New Results in Hadronic Interactions,* Proceedings of the XXIVth Rencontre de Moriond, Les Arcs, France, 1989, edited by J. Tran Thanh Van (Editions Frontieres, Paris, 1989), p. 273.

[11] P. Carruthers, Astrophys. J. **380**, 24 (1991).

[12] W. Goodman, *Statistical Optics* (Wiley, New York, 1986).

[13] F. Takagi, Phys. Rev. Lett. **53**, 427 (1984); Phys. Rev. C **32**, 1799 (1985).

[14] Recall that the final-state hadrons may have various quantum numbers and massses. For simplcity, we restrict our analysis to one species of particle of common mass m. Since the transverse momentum $p_\perp$ is fairly small compared to p_z along the collision axis, it is convenient to suppress the $p_\perp$ dependence and to describe the longitudinal momentum in terms of the rapidity variable y: $y=\frac{1}{2}\ln(E+p_z)/(E-p_z)$, $E=m_\perp\cosh y$, $p_z=m_\perp\sinh y$, where $m_\perp=(p_\perp^2+m^2)^{1/2}$ is the usual "transverse mass." Under changes of reference along the z axis, y is an additive variable. A standard theoretical world is the one at infinite energy with flat rapidity density $\rho_1(y)$ and translation-invariant correlation functions of all orders. In reality, one has to live with "central regions," in which $\rho_1(y)$ is not necessarily as flat as one might wish and for which the entire spread ΔY of the histogram is 4–10 units of rapidity. In any case, we shall restrict our analysis to the "central region" in order to make use of the well-known mathematical apparatus of stationary processes. Kinematically, the c.m. rapidity of a particle is bounded by $y_{\max}=\ln(2E/m_\perp)$, which in turn must be less than or equal to $\ln(W/m_\perp)$, W the total c.m. energy.

[15] UA5 Collaboration, Z. Phys. C **43**, 357 (1989); Phys. Lett. **160B**, 193 (1985).

[16] NA22 Collaboration, I. V. Ajinenko *et al.,* Phys. Lett. **22B**, 306 (1989); M. Adamus *et al.,* Z. Phys. C **37**, 215 (1988).

[17] T. Hakioğlu, in *Intermittency in High Energy Collisions,* Proceedings of the Santa Fe Workshop, Los Alamos, New Mexico, 1990, edited by F. Cooper, R. C. Hwa, and I. Sarcevic (World Scientific, Singapore, 1991); University of Arizona, Ph.D. thesis, 1991.

[18] P. Carruthers, H. C. Eggers, and I. Sarcevic, Phys. Lett. B **254**, 258 (1991).

[19] P. J. E. Peebles, *The Large-Scale Structure of the Universe* (Princeton University Press, Princeton, NJ, 1980).

[20] P. Grassberger and I. Procaccia, Phys. Rev. Lett. **50**, 346 (1983).

[21] I. M. Dremin, Mod. Phys. Lett. A **3**, 1333 (1988).

[22] E. P. Wigner, Phys. Rev. **40**, 749 (1932); P. Carruthers and F. Zachariasen, Rev. Mod. Phys. **55**, 245 (1983).

[23] A. Arneodo, Phys. Rev. Lett. **61**, 2281 (1988).

[24] B. Durand and L. O'Raifeartaigh, Phys. Rev. D **13**, 99 (1976).